PHYSICAL REVIEW LETTERS **98**, 197402 (2007)
Preprint of accepted version.
File generated by M. Hoffmann on 17.01.2008.

Single-Step Triplet-Triplet-Annihilation: An Intrinsic Limit for the High-Brightness Efficiency of Phosphorescent Organic Light Emitting Diodes.

W. Staroske,* M. Pfeiffer, K. Leo, and M. Hoffmann†
Institut für Angewandte Photophysik, Technische Universität Dresden, D-01062 Dresden, Germany

We investigate triplet-triplet-annihilation in molecular host-guest systems where triplets are localized on spatially separated guest molecules. Our results indicate that the dominant mechanism of annihilation is single-step long-range (Förster-type) energy transfer between two excited guests. This mechanism leads to a fundamental limit for the efficiency of phosphorescent organic light emitting diodes at high luminance. Our model is confirmed by photoluminescence decay experiments on 2,3,7,8,12,13,17,18-octaethylporphine platinum as guest in a host-matrix of 4,4′-N,N′-dicarbazole-biphenyl.

Organic light emitting diodes (OLED) have broad applications perspectives in displays and lighting. Recently, very high efficiency devices have been realized, based on phosphorescent emitters [1] and pin-structures with doped transport layers [2]. In those devices, host-guest systems with phosphorescent guest molecules are employed to harvest the triplet excitons created from statistical charge recombination. Typical triplet emitters are the organometallic phosphors 2,3,7,8,12,13,17,18-octaethylporphine platinum (PtOEP) and *fac* tris(2-phenylpyridine) iridium ($Ir(ppy)_3$) [3]. In particular with $Ir(ppy)_3$ emitters, internal quantum efficiencies close to unity have been achieved [4]. At high exciton densities, however, the intrinsically high efficiency of phosphoresent OLED is counteracted by strong bimolecular annihilation processes. This leads to a roll-off of the quantum efficiency and thus brightness (luminance) at high driving currents [5], which is very detrimental for high-brightness display and lighting applications.

Bimolecular recombination is most important for long-living states. In principle, all possible pairs of triplets or single charge carriers (polarons) on host or guest molecules can lead to bimolecular annihilation reactions. Baldo and coworkers [5, 6] have comprehensively discussed these effects by comparing electroluminescence (EL) and photoluminescence (PL) data for a variety of host-guest combinations and concluded that bimolecular annihilation is best suppressed when triplets are trapped on the guests. This is fulfilled for the model system of PtOEP as guest in a host-matrix of the amorphous, hole transporting wide-gap organic semiconductor 4,4′-N,N′-dicarbazole-biphenyl (CBP).

However, even for this case, pronounced bimolecular annihilation was observed in EL and in PL [5, 6]. In particular in PL, the process of triplet generation can be clearly identified: photoexcitation of the CBP host creates singlets in the host. These transfer to singlets in the PtOEP guest where they transform to guest triplets by intersystem crossing. When discussing the unexpected annihilation, Baldo et al. [5] nevertheless rule out direct guest-guest annihilation and argue qualitatively that host triplets must be present, although their presence could not be understood in the present models.

In this Letter, we present an alternative explanation for annihilation of guest triplets: single-step long-range Förster-type energy transfer between two excited guest molecules, i.e. a reaction of the type $T_1 + T_1 \rightarrow S_0 + T_n$. Although this type of energy transfer involves a spin-flip in the donor ($T_1 \rightarrow S_0$) and therefore is intrinsically slow, it only competes with the slow radiative recombination rate of the donor, which requires the same spin-flip. The resulting interaction radius R_F is entirely determined by the overlap integral between normalized donor emission and the absorption coefficient of the acceptor transition $T_1 \rightarrow T_n$. Since $T_1 \rightarrow T_n$ is spin-allowed, R_F can have as large values as for triplet-singlet [7] or for the well known singlet-singlet transfer. Triplet-triplet annihilation of this type has already been clearly described by Kellogg [8] for phenanthrene in liquid solution, and Förster radii of the order of 4 nm have been both predicted and measured.

To prove our explanation, we performed PL decay measurements with PtOEP-doped CBP similar to Ref. [5]. We analyzed them with the general rate equation for the density n of guest triplets of intrinsic lifetime τ:

$$\frac{d}{dt}\, n(t) = -\frac{n(t)}{\tau} - f\gamma n(t)^2 \,. \qquad (1)$$

Here, γ is the annihilation rate constant, and the factor f depends on the final product of the annihilation reaction. If one exciton survives ($T_n \rightarrow T_1$), f becomes $\frac{1}{2}$ but otherwise $f = 1$ (e.g. [6, 9]). We always assume $\frac{1}{2}$.

For empirical analysis of annihilation experiments, it is common to consider γ as a constant [5, 6, 10]. This results from the microscopic model of a three-dimensional diffusion-controlled reaction, where after some short initial time interval γ takes the form of $\gamma_0 = 8\pi Da$, with diffusion constant D and annihilation distance a [11].

The rate limiting process in this model is the motion of excitons towards each other, which takes place in the form of many single excitation transfer steps of the type $T_1 + S_0 \rightarrow S_0 + T_1$. This means, the exciton performs a multi-step random walk on the grid of unexcited guests.

In our alternative approach, we neglect the multi-step motion of excitons via *unexcited* guests and consider only single steps between two *excited* guests ($T_1 + T_1 \rightarrow S_0 + T_n$). The most efficient long-range interaction is dipole-dipole coupling (Förster transfer). From the decay law derived by Förster [12] for an excited donor statistically surrounded by acceptors, the annihilation rate constant after a short excitation pulse at $t = 0$ can be approximated as [9]

$$\gamma(t) = \frac{2}{3}\pi R_{\mathrm{F}}^3 \sqrt{\frac{\pi}{\tau t}}\,. \tag{2}$$

Here, R_{F} is the Förster radius for transfer to an excited guest. In remarkable contrast to a diffusion controlled reaction, there is no regime in which γ becomes time-independent. With γ from Eq. (2) and initial condition $n(t = 0) = n_0$, the general rate equation (1) is solved by

$$n(t) = \frac{n_0\, e^{-t/\tau}}{1 + \frac{2}{3}\pi^2 f n_0 R_{\mathrm{F}}^3 \operatorname{erf}\left(\sqrt{\frac{t}{\tau}}\right)}. \tag{3}$$

This decay law is used for our analysis of the PL annihilation experiments.

Our samples were prepared in high-vacuum by coevaporation of gradient sublimated CBP and PtOEP onto fused silica. Excitation for time-resolved PL was done with the central (and thus homogeneous) part of an unfocused beam from a pulsed nitrogen laser at 337 nm. The emission was filtered by a 620 nm long pass filter, imaged onto a photo diode and recorded by a digital oscilloscope. Measurements where done under ambient conditions directly after sample preparation. Then, sample degradation was still negligible as inferred from the mono-exponential decay at low excitation densities.

To fit the decay law (3) to the experimental PL decay curves, we assume an initial exciton distribution along the optical path x in the sample given by Beer's law: $n_0(x) = n_{00} \exp(-\alpha x)$. Integration over x gives an equation for the total PL signal $L(t)$, which has as free parameters only a scaling factor L_0 (for detection efficiency) and R_{F}. As intrinsic lifetime, $\tau = 95\,\mu$s was taken from mono-exponential fits at low excitation density. For the initial density n_{00} at the front interface, the density n_{ex} of singlets created in the host was obtained from the measured pulse energy and the absorption coefficient. Optical constants where obtained from fitting thin-film optical models to a set of transmission and reflection data of various thickness as in Ref. [13].

The efficiency η_{hg} of singlet transfer from host to guest was obtained from comparing the guest luminescence for excitation of either host or guest singlets at their respective absorption maxima. The transfer efficiencies at low excitation ranged from 52 % for a guest concentration of 0.13 mol% to 87 % for 1.8 mol%.

For the intersystem crossing efficiency η_{ISC} in the guest molecules, we assumed 100 % based on the following arguments: Ponterini et al. [14] measured the total decay time of the S_1 state of PtOEP to be smaller than 15 ps and estimated the radiative lifetime to 60 ns. The nonradiative decay rate constant can be estimated from the fluoresence quantum yield of ~ 0.16 in the related free base compound H_2OEP [15]. This yields intersystem crossing efficiencies of at least 99 %. Then, the created triplet density follows as $n_{00} = n_{\mathrm{ex}}\eta_{\mathrm{hg}}\eta_{\mathrm{ISC}}$. In the low excitation intensity regime, the calculated initial triplet density n_{00} was proportional to the initial PL signal $L(0)$. This proportionality constant was used to determine n_{00} from $L(0)$ in the high excitation density regime, where host singlet annihilation or guest saturation may start.

In Fig. 1, we show examples of PL decay and fit residues for two different initial concentrations n_{00} in the sample of highest guest concentration 1.8 mol%. For comparison, we also show fit results based on the multi-step diffusion model with a constant γ_0 in Eq. (1). The residues clearly show that our single-step model gives a more accurate description of the decay curves [16].

Figure 2 shows all fitted Förster radii R_{F}. For each guest concentration, R_{F} is independent of n_{00} over a large range, as it should be in this model. If n_{00} becomes very large, it reaches the density of available guest molecules visualized by vertical lines. Then, the formally obtained values of R_{F} drop down since in this saturation regime the data show a fast initial decay which cannot be properly described by the model anymore. The increase of R_{F} for $n_{00} < 3 \times 10^{17}\,\mathrm{cm}^{-3}$ is an artefact from the fitting procedure since then the actual annihilation term is very small and cannot be properly extracted anymore.

The result of a constant R_{F} versus n_{00} is not trivial, since a variation of n_{00} varies the average distance of excitons, and annihilation depends on the relation of this distance to the characteristic length of exciton transfer given by R_{F}. Furthermore, Figure 2 shows that R_{F} does not depend on the guest concentration, which means that the distance of unexcited guests is not relevant. This is the crucial support of our hypotheses that annihilation involves only exciton transfer between excited guests.

The empirical Förster radius obtained for the whole set of exciton and guest molecule concentrations is in the range $R_{\mathrm{F}} = (5.20 \pm 0.08)$ nm. Evaluation in the framework of multi-step diffusion models results in values of $\gamma_0 = (8 \pm 1) \times 10^{18}\,\mathrm{cm}^3\mathrm{s}^{-1}$, which do not vary with guest concentration. A constant γ_0 versus guest concentration is in strong contradiction to the underlying model of diffusion on the grid of guest molecules, where the diffusion constant should strongly depend on the average guest distance.

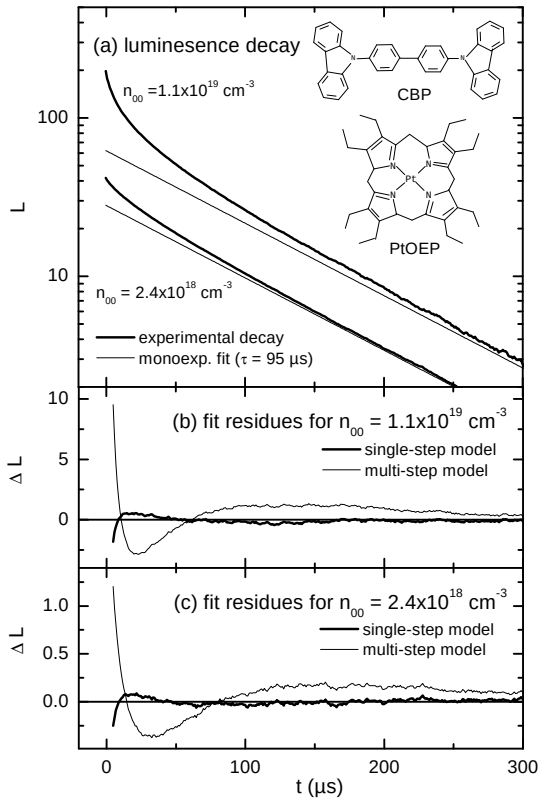

FIG. 1: (a) Experimental decay of luminescence signal $L(t)$ and mono-exponential fits for the sample with highest investigated guest concentration at two initial front-face triplet densities n_{00}. Excitation energy densities were $1.2\times10^{-4}\,\mathrm{J\,cm^{-2}}$ and $1.4\times10^{-5}\,\mathrm{J\,cm^{-2}}$. (b) Fit residues at $n_{00}=1.1\times10^{19}\,\mathrm{cm^{-3}}$ for fits with the single-step Förster transfer model ($R_\mathrm{F}=5.2\,\mathrm{nm}$) and the multi-step diffusion model ($\gamma_0=9.0\times10^{-15}\,\mathrm{cm^3s^{-1}}$). (c) Fit residues at $n_{00}=2.4\times10^{18}\,\mathrm{cm^{-3}}$ for the single-step model ($R_\mathrm{F}=5.2\,\mathrm{nm}$) and the multi-step model ($\gamma_0=8.5\times10^{-15}\,\mathrm{cm^3s^{-1}}$). The fit curves are not shown in panel (a) since they entirely coincide with the experimental curves on this scale.

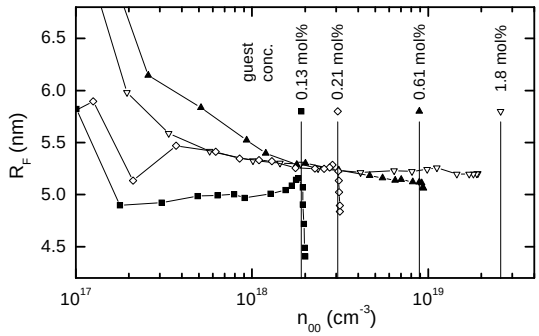

FIG. 2: Fit results for the Förster radius R_F versus initial front-face triplet concentration n_{00} for four different samples with different mol:mol concentration of guest molecules. The density of guest molecules in each sample is shown by vertical lines.

From a microscopic viewpoint, the Förster radius R_F depends on the spectral overlap of the donor emission spectrum $F_\mathrm{D}(\tilde\nu)$ (normalized to PL quantum efficiency) and the spectrum of the acceptor molar extinction coefficient $\epsilon_\mathrm{A}(\tilde\nu)$ (from [17]):

$$R_\mathrm{F}^6=\frac{9\ln10\,\kappa^2}{128\pi^5N_An_\mathrm{r}^4}\int F_\mathrm{D}(\tilde\nu)\epsilon_\mathrm{A}(\tilde\nu)\frac{d\tilde\nu}{\tilde\nu^4}\,. \qquad (4)$$

Here, κ is the directional factor taken to be $\kappa^2=2/3$ and n_r is the refractive index of the matrix (here $n_\mathrm{r}=1.7$).

Transient absorption spectra of PtOEP [14] show strong $\mathrm{T}_1\rightarrow\mathrm{T}_n$ transitions in the wavelength region 550-800 nm. A quantitative estimate can be made from the absolute $\mathrm{T}_1\rightarrow\mathrm{T}_n$ extinction coefficient measured in Ref. [18] for the photophysically very similar zinc tetraphenylporphine (ZnTPP). In the PtOEP emission range (FWHM 21 nm around 647 nm), this extinction coefficient is nearly constant $3.5\times10^3\,\mathrm{l\,mol^{-1}cm^{-1}}$ [18]. With this constant value, Eq. (4) gives a Förster radius of 3.6 nm. This estimate indicates that the order of magnitude of the Förster radius derived from our fits (5.2 nm) is reasonable. As for the case of $\mathrm{Ir(ppy)_3}$ discussed below, the higher value (i.e. stronger annihilation) from the experimental evaluation is most likely caused by partial aggregation, maybe even with a preferentially parallel orientation of transition dipoles, in contrast to the assumptions for Eq. (4).

The single-step annihilation mechanism sets an intrinsic limit to the internal quantum efficiency of OLEDs at high exciton concentrations. To estimate this limit, we calculate the relative quantum efficiency $\Phi=\left(\int n(t)dt\right)/\left(\int n_0\mathrm{e}^{-t/\tau}dt\right)$ with $n(t)$ from Eq. (3). Φ depends only on the dimensionless product

$$\xi=\frac{2}{3}\pi^2fn_0R_\mathrm{F}^3\,, \qquad (5)$$

and numerical solution of $\Phi(\xi_\mathrm{c})=\frac{1}{2}$ gives the critical value $\xi_\mathrm{c}=1.516$ at which the relative quantum efficiency drops to $\frac{1}{2}$. For the $R_\mathrm{F}=5.2\,\mathrm{nm}$ obtained in our fits, the critical initial concentration in the pulsed regime becomes $n_{0\mathrm{c}}=3.3\times10^{18}\,\mathrm{cm^{-3}}$.

To get an order-of-magnitude estimate for the case of a stationary exciton creation rate $\dot n=\chi j/(ed)$ in an OLED with exciton yield χ due to spin-statistics (here $\chi=1$) and generation layer thickness d, we assume that first annihilation is "turned off" and a stationary exciton density $\chi j\tau/(ed)$ is created. Now, starting from this initial state, creation is "turned off" and annihilation is "turned on". Then, the effect of annihilation on the originally created exciton density can be seen [19]. In this way, the critical current density j_c for a quantum-efficiency roll-off to $\frac{1}{2}$ can be obtained from the critical density $n_{0\mathrm{c}}$ in the pulsed regime and Eq. (5):

$$j_\mathrm{c}=\frac{3\xi_\mathrm{c}ed}{2\pi^2f\chi R_\mathrm{F}^3\tau}\,. \qquad (6)$$

With $d = 10\,\mathrm{nm}$ as in [5], we get for a PtOEP guest emitter device $j_\mathrm{c} = 5\,\mathrm{mA/cm^2}$. This corresponds well to the experimental result in Ref. [5], where j_c is in the range $1 - 4\,\mathrm{mA/cm^2}$. Even the remaining trend in Ref. [5] is reasonable: The smallest j_c occurs at the smallest guest concentration, where also the overall quantum efficiency is reduced showing that the actually created triplet concentrations are lower. The alternative multi-step model, however, would suggest a higher j_c (impeded annihilation) for small guest concentrations.

Assuming an internal quantum yield limited by 50% PL quantum yield [20] and a Lambertian emitter with a typical outcoupling efficiency of 20% [4], our j_c corresponds to a critical roll-off luminance of $340\,\mathrm{cd/m^2}$, which is just within typical display range. This is the fundamental limit for any OLED with statistically distributed PtOEP emitters if one does not succeed to increase the generation layer width above 10 nm, e.g., by employing double-emission layers [21].

As in multi-step models, the critical current density j_c in the single-step model can be increased by decreasing the lifetime τ of the emitter. This trend is used by improved OLED emitter materials like $\mathrm{Ir(ppy)_3}$ [3], which indeed show drastically increased j_c up to $0.6\,\mathrm{A/cm^2}$ [5]. If we estimate R_F for single-step annihilation using the $\mathrm{Ir(ppy)_3}$ excited state extinction coefficient of $\sim 1.3 \times 10^3\,\mathrm{l\,mol^{-1}cm^{-1}}$ [22], we get $R_\mathrm{F} = 2.9\,\mathrm{nm}$ and with $\tau \sim 0.5\,\mu\mathrm{s}$ the critical current density becomes $j_c \sim 6\,\mathrm{A/cm^2}$. The experimental j_c from Ref. [5] is much lower than this limit. We assume that $\mathrm{Ir(ppy)_3}$ in coevaporated layers has a much stronger tendency of aggregate formation than PtOEP, which leads to a larger fraction of short-distance exciton pairs with strong annihilation. Aggregation is clearly prevented in the $\mathrm{Ir(ppy)_3}$-related systems with dendrimeric spacers described by Namdas et al. [10]. For large spacers, indeed a critical current density of $18\,\mathrm{A/cm^2}$ [23] is derived from PL annihilation experiments. This agrees reasonably with our estimate from approximate excited state absorption values. Interestingly, Namdas et al. [10] find increasing annihilation for smaller spacers (center-center distance $< 2\,\mathrm{nm}$), which contradicts to our single-step model. For such small distances, multi-step diffusion through Dexter transfer becomes the dominant annihilation process [10].

In conclusion, we have proposed a new explanation for the OLED efficiency roll-off, which calls for new optimization strategies: Besides short lifetime and effective separation of the guest molecules, minimization of the spectral overlap between $\mathrm{T_1} \rightarrow \mathrm{S_0}$ emission and $\mathrm{T_1} \rightarrow \mathrm{T}_n$ absorption is required.

We thank Z. G. Soos for inspiring discussions and a very useful hint regarding the application of the Förster equation to the annihilation problem, and T. Fritz for help with thin-film optics and experimental questions. Financial support by Deutsche Forschungsgemeinschaft (Leibnizpreis) is gratefully acknowledged.

* Present address: Institut für Biophysik, Technische Universität Dresden, Germany
† Present address: Fraunhofer IPMS, Dresden, Germany; Electronic address: Michael.Hoffmann@ipms.fraunhofer.de

[1] M. A. Baldo, D. F. O'Brien, Y. You, A. Shoustikov, S. Sibley, M. E. Thompson, and S. R. Forrest, Nature **395**, 151 (1998).
[2] G. He, M. Pfeiffer, K. Leo, M. Hofmann, J. Birnstock, R. Pudzich, and J. Salbeck, Appl. Phys. Lett. **85**, 3911 (2004).
[3] M. A. Baldo, M. E. Thompson, and S. R. Forrest, Pure Appl. Chem. **71**, 2095 (1999).
[4] C. Adachi, M. A. Baldo, M. E. Thompson, and S. Forrest, J. Appl. Phys. **90**, 5048 (2001).
[5] M. A. Baldo, C. Adachi, and S. R. Forrest, Phys. Rev. B **62**, 10967 (2000).
[6] M. A. Baldo and S. R. Forrest, Phys. Rev. B **62**, 10958 (2000).
[7] M. A. Baldo, M. E. Thompson, S. R. Forrest, Nature **403**, 750 (2000).
[8] R. E. Kellogg, J. Chem. Phys. **41**, 3046 (1964).
[9] E. Engel, K. Leo, and M. Hoffmann, Chem. Phys. **325**, 170 (2006).
[10] E. B. Namdas, A. Ruseckas, I. D. W. Samuel, S.-C. Lo, and P. L. Burn, Appl. Phys. Lett. **86**, 091104 (2005).
[11] R. C. Powell and Z. G. Soos, J. Lum. **11**, 1 (1975).
[12] T. Förster, Z. Naturforsch. **4a**, 321 (1949).
[13] A. B. Djurisic, T. Fritz, and K. Leo, Optics Communications **166**, 35 (1999).
[14] G. Ponterini, N. Serpone, M. A. Bergkamp, and T. L. Netzel, J. Am. Chem. Soc. **105**, 4639 (1983).
[15] V. S. Chirvony, A. van Hoek, V. A. Galievsky, I. V. Sazanovich, T. J. Schaafsma, and D. Holten, J. Phys. Chem. B **104**, 9909 (2000).
[16] We have checked that even inclusion of the transient term $\propto 1/\sqrt{Dt}$, see e.g. [11], in γ_0 does not improve the fit with the multi-step model significantly.
[17] J. B. Birks, *Photophysics of Aromatic Molecules* (Wiley-Interscience, London, 1970).
[18] L. Pekkarinen and H. Linschitz, J. Am. Chem. Soc. **82**, 2407 (1960).
[19] In contrast to annihilation models with time-independent γ, the single-step Förster model allows no direct transition to the stationary regime by setting $\dot{n} = 0$.
[20] D. B. Papkovsky, Sensors Actuators B **29**, 213 (1995).
[21] X. Zhou, D. S. Qin, M. Pfeiffer, J. Blochwitz-Nimoth, A. Werner, B. M. J. Drechsel, K. Leo, M. Bold, P. Erk, and H. Hartmann, Appl. Phys. Lett. **81**, 4070 (2002).
[22] K. Ichimura, T. Kobayashi, K. A. King, and R. J. Watts, J. Phys. Chem. **91**, 6104 (1987).
[23] Ir-G2 value from [10] scaled to $d = 10\,\mathrm{nm}$.